

Ultrafast carrier dynamics in semiconductor quantum dots

V. Klimov,* P. Haring Bolivar, and H. Kurz

Institut für Halbleitertechnik II, Rheinisch Westfälische Technische Hochschule Aachen, Sommerfeldstrasse 24, D-52074 Aachen, Germany

(Received 24 May 1995; revised manuscript received 25 September 1995)

The dynamics of band-edge photoluminescence (PL) in CdS nanocrystals (NC's) dispersed in a glass matrix are studied with the femtosecond up-conversion technique. The time-resolved PL spectra exhibit several discrete features (three of them are in the NC energy band gap) which are not pronounced in a cw PL spectrum. The initial stage of a PL decay is governed by a depopulation of the lowest extended states due to carrier trapping (localization) on the time scale of 1 ps. The low-energy bands originating from the extended-to-localized state transitions exhibit extremely fast buildup dynamics (rise time is 400–700 fs) which is explained by the preexisting occupation of the localized states.

I. INTRODUCTION

Semiconductor nanocrystals (NC's) grown in a glass matrix¹ or prepared chemically either in a polymer film or as colloids² represent a class of quasi-zero-dimensional systems or quantum dots. These objects exhibit size-dependent absorption and photoluminescence (PL) spectra which result from three-dimensional (3D) carrier confinement. Large and fast optical nonlinearities^{3,4} as well as lasing⁵ reported for these materials make them attractive for potential applications in optoelectronics and signal processing.

Linear and nonlinear absorption studies^{4,6} are usually applied to derive the structure of delocalized volume states in NC's which carry significant oscillator strengths. On the other hand, PL studies demonstrate the important role of states in the NC energy band gap associated with the surface and/or defects.^{7–10} These states correspond to localized carriers and are not well resolved in absorption. The PL spectra of CdS, CdSe, and CdS_xSe_{1-x} NC's usually consist of two broad bands: One (high energy) at the band-edge spectral energies and the other (low energy) in the near-IR–red spectral range.^{10–13} The low-energy band has been suggested to originate from donor-acceptor recombination involving deep defect states associated with sulfur vacancies.^{7,8} The high-energy band (band-edge emission) has been explained by different recombination mechanisms, such as recombination of the delocalized electron-hole (*e-h*) pairs strongly coupled to lattice vibrations¹⁴ or recombination through localized states, possibly, of surface origin.^{10,15,16} The relaxation of the band-edge PL is characterized by fast and usually multiexponential dynamics (on the ns or ps time scales) (Refs. 10, 12, 13, and 17) which can be strongly affected by “photodarkening.”¹⁸ The fastest components of PL have been explained in terms of the nonradiative Auger recombination¹⁷ or carrier trapping.^{13,18,19} Femtosecond pump-probe^{20–22} and photon-echo²³ measurements show that the relaxation times relating to the population changes in NC's can be on the time scale of a few ps or less. This demonstrates the important role of direct femtosecond measurements in the study of carrier dynamics in semiconductor NC's.

In the present paper we report a femtosecond study of the band-edge emission in CdS NC's performed by the lumines-

cence up-conversion technique.²⁴ The time-resolved PL spectra exhibit several discrete features, some of which are in the NC energy band gap. This indicates the presence of shallow localized states involved in the band-edge emission. The subpicosecond and picosecond PL dynamics studied are explained in terms of carrier cooling and subsequent trapping into localized states.

II. EXPERIMENTAL PROCEDURE

The samples under investigation are CdS NC's grown in a glass matrix by the method of the secondary heat treatment.¹ The average NC radius estimated from the position of the absorption edge is approximately 4 nm. The samples are excited at 3.1 eV by frequency-doubled 100-fs pulses from a mode-locked Ti:sapphire laser. The luminescence from the sample is mixed in a nonlinear β -barium borate crystal with variably delayed pulses at a fundamental frequency of the Ti:sapphire laser to generate a sum-frequency signal in the near-UV spectral region. The up-converted signal is dispersed by a monochromator and is finally detected by a cooled photomultiplier. The zero delay is found by recording a cross-correlation trace between the scattered pump light from the sample and a delayed laser pulse at a fundamental frequency used for PL up conversion. The spectral resolution of the system is 20 meV, and the time resolution is around 200 fs. To avoid the transient changes in carrier dynamics resulting from photochemical effects the excited spot of the sample has been initially “darkened” by strong laser illumination for sufficient duration. In all measurements reported below, the pump intensity has been intentionally kept at a level $I_p < 20$ mW (pump fluence $w_p < 10 \mu\text{J cm}^{-2}$) corresponding to the excitation of less than one electron-hole pair per NC on average. This allows us to avoid the saturation of trap states and effects of fast Auger recombination which might complicate the interpretation of the experimental data. All measurements are performed at room temperature.

III. EXPERIMENTAL RESULTS

Time-resolved spectra of the band-edge emission of CdS NC's recorded at different delay times are shown in Fig. 1 (solid lines) along with a cw (time-integrated) spectrum

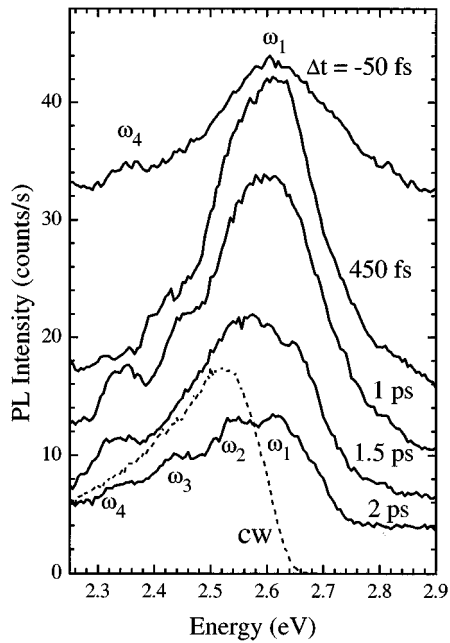


FIG. 1. Time-resolved (solid lines) and cw (dashed line) PL spectra of CdS NC's measured at pump fluence $w_p = 5 \mu\text{J cm}^{-2}$ (to avoid intersections the spectra are arbitrarily shifted along the vertical axis).

(dashed line) taken at the same pump intensity. The up-converted PL spectra exhibit a number of discrete features which are not resolved in the cw spectrum. These features are denoted in Fig. 1 as ω_i ($i = 1-4$). Band ω_1 is located at the position of the lowest optical transition derived from the absorption data. Band ω_2 is redshifted by about 80 meV; its maximum coincides with a maximum of the cw PL. Two other bands (ω_3 and ω_4) are shifted further to the low-energy side of the ω_1 band by ~ 170 and ~ 270 meV, respectively. The striking feature of the recorded spectra is the extremely fast buildup dynamics in the whole spectral range. The low-energy band ω_4 is clearly seen along with the high-energy ω_1 band already at negative delay times. The up-converted PL is dominated by the ω_1 band at small delay times $\Delta t < 1$ ps. At longer delays the maximum of PL shifts to the ω_2 line which dominates the cw band-edge emission. The initial relaxation time of spectrally integrated PL derived from the spectra in Fig. 1 is ~ 1 ps.

To study in detail the buildup and the fast-relaxation dynamics we have recorded the PL intensity at fixed spectral positions by varying the delay time with a small step (50 fs) in the range up to 6 ps. The results of these measurements (Fig. 2) have been used to derive the rise time τ_r and the fast-relaxation time τ_1 by fitting to a function $y = y_0 + A(1 - e^{-(t-t_0)/\tau_r})e^{-(t-t_0)/\tau_1}$. The spectral distributions of these times are shown in Fig. 3. For high photon energies ($\hbar\omega > 2.85$ eV), the PL rise time appears to be limited by our time resolution. At spectral energies 2.7–2.8 eV the time τ_r reaches the values of 400–500 fs. It slightly increases up to 700–800 fs in the region 2.6–2.7 eV and remains nearly constant (500–600 fs) at the lower spectral energies (2.3–2.5 eV).

The relaxation of PL is nearly exponential at photon energies $\hbar\omega > 2.75$ eV. The relaxation time increases from

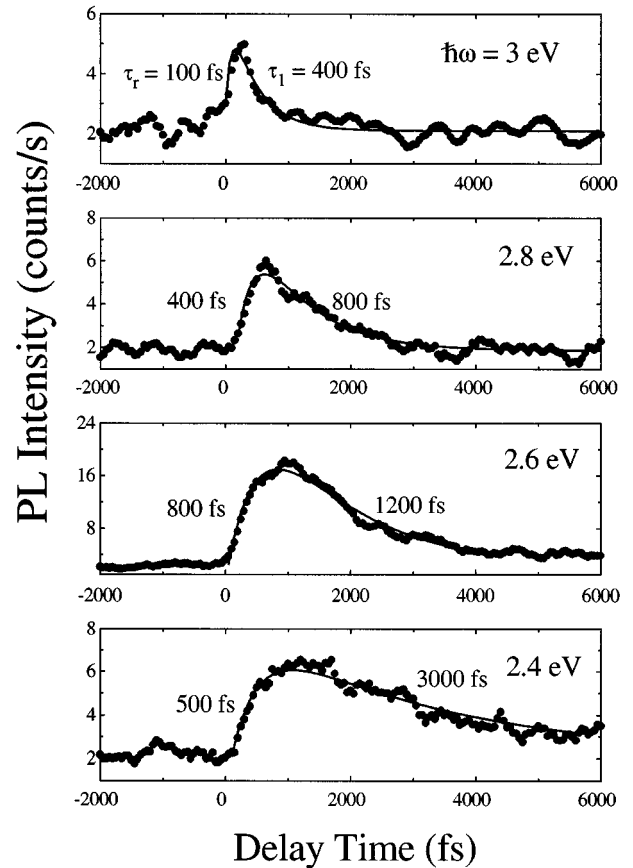


FIG. 2. The time evolution of the PL intensity at different spectral energies (short-scan measurements). Symbols are the experimental data; lines are fits to a function $y = y_0 + A(1 - e^{-(t-t_0)/\tau_r})e^{-(t-t_0)/\tau_1}$.

~ 400 fs at 3 eV up to 800–900 fs at 2.75 eV. At lower spectral energies, the fitting procedure shows the presence of the nonzero offset that is indicative of an additional slower component in the PL decay. To derive the relaxation times of

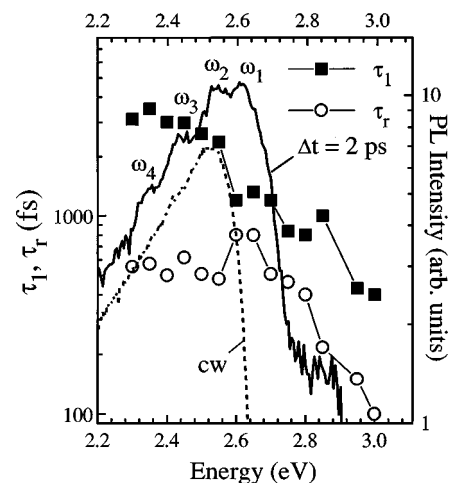


FIG. 3. Spectral distributions of the rise time (circles) and the fast-relaxation time (squares) of PL (derived from the data of the short-scan measurements) in comparison to the cw (dashed line) and the up-converted (solid line) PL spectra. The up-converted spectrum is taken at $\Delta t = 2$ ps.

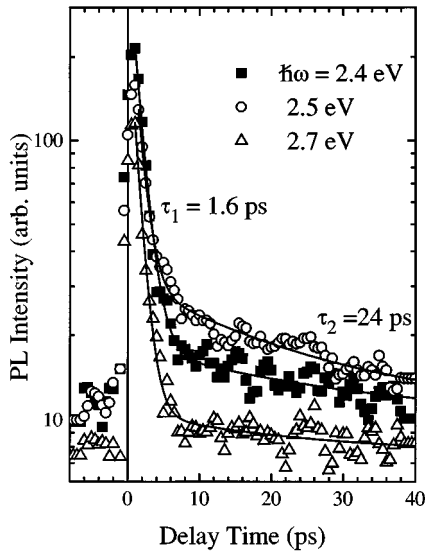


FIG. 4. The time evolution of the PL intensity at different spectral energies (long-scan measurements). Symbols are the experimental data; lines are fits to the two-exponential decay.

this component we have performed long-scan measurements with Δt being varied up to 50 ps with a step of 0.5 ps (Fig. 4). All transients taken can be fitted to the two-exponential decay with relaxation times being only slightly dependent on the spectral energy in the whole range from 2.3 to 2.7 eV. The fast-relaxation constant (τ_1) is 1–3 ps and the slow one (τ_2) is 20–30 ps. The improved data for the short-lived component derived from the short-scan measurements are (see Fig. 3) ~ 1.2 ps (2.6–2.7 eV), 2.5–3.5 ps (2.3–2.55 eV). The spectral distributions of the amplitudes of the fast and slow components in the PL decay (Fig. 5) correlate with the features observed in the time-resolved PL spectra. The fast component is peaked at the positions of the ω_1 and ω_3 bands, whereas the slow component reaches the maximum in the range of the ω_2 band and shows a step at the position of the ω_4 band.

The two-exponential carrier decays with nearly the same time constants as those measured by us have been previously

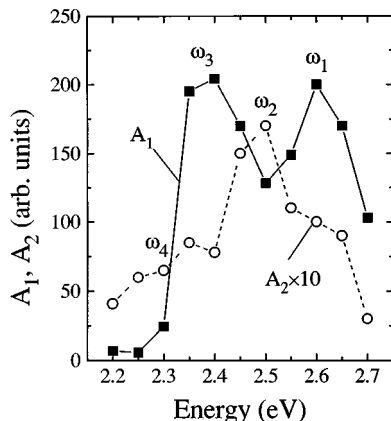


FIG. 5. Spectral distributions of the amplitudes for the fast A_1 (squares) and the slow A_2 (circles) components in the PL decay (derived from the data of the long-scan measurements).

reported for CdS (Ref. 22) and $\text{Zn}_{1-x}\text{Cd}_x\text{S}$ (Ref. 25) colloids and explained in terms of Auger recombination. In our measurements, this process can be definitely ruled out because the average number of the $e-h$ pairs per NC is less than one. In the case of strong inhomogeneous broadening expected for the samples under investigation, a size-dependent carrier relaxation could lead to the nonexponential PL decay. However, this would be manifested as a certain spectral distribution of relaxation times which is not observed. The transients taken in the whole spectral range under investigation can be correctly fitted by using three well-defined relaxation times. We believe that the nonexponential decay observed arises from the overlap of the neighboring transitions with different relaxation dynamics. These transitions are associated with the ω_1 – ω_4 bands (see Figs. 1 and 5). The analysis of the relaxation dynamics performed shows that transitions ω_2 and ω_4 have relatively slow and nearly the same relaxation dynamics with time constant 20–30 ps, whereas the transitions ω_1 and ω_3 are characterized by much shorter relaxation times of about 1 and 3 ps, respectively.

IV. DISCUSSION

The spectra in Fig. 1 as well as the literature data on the band-edge emission in CdS, CdSe, and $\text{CdS}_x\text{Se}_{1-x}$ quantum dots prepared by different techniques show a redshift of the cw-PL maximum by several tens of meV of the lowest absorption peak. This shift has been explained either by strong electron-phonon interaction¹⁴ or by the presence of localized states (surface and/or defect) involved in the band-edge emission.¹⁶ In the femtosecond spectra shown in Fig. 1 we have observed both maxima: One (short-lived) at the transition between the lowest extended states (ω_1), and the other (long-lived) at the position of the cw-emission maximum (ω_2). This observation excludes an explanation of the PL redshift by strong coupling of extended states to lattice vibrations and clearly shows the presence of the localized states in the energy band gap which are involved in the band-edge emission.

We now analyze the relation between the dynamics on the buildup and the relaxation at different spectral energies. The relaxation of the PL intensity at 3 eV is complementary to the PL buildup dynamics at 2.6 eV (see Figs. 2 and 3). This can be explained in terms of carrier cooling during intraband energy relaxation. The average energy-loss rate estimated from the data shown is about 0.7 meV fs^{-1} per $e-h$ pair, that is, on the order of the cooling rate expected for the unscreened polar carrier-phonon interaction in bulk CdS and several times larger than the experimentally measured values for the bulk material at the same pump intensities.²⁷ As shown in Ref. 27, the slowed cooling in bulk CdS is chiefly caused by the hot-phonon effects (see, e.g., Ref. 28) which evidently have reduced efficiency in quantum-dot systems. The fast carrier cooling observed by us is consistent with data on carrier relaxation dynamics in CdSe and $\text{CdS}_x\text{Se}_{1-x}$ quantum dots obtained by using femtosecond pump-probe measurements of nonlinear transmission.^{20,21}

Surprisingly, we did not observe the slowing down of the buildup dynamics for the low-energy part of the PL spectra which might be attributed to the carrier localization (see picosecond data on the PL buildup dynamics in Ref. 29). This

could mean an extremely fast carrier trapping from the ground extended states (with a time constant shorter than 200 fs) as suggested in Refs. 15, 20, and 23. However, this is not consistent with a measured relaxation time ($\tau_1 = 1.2$ ps) of the ω_1 band associated with transition coupling the lowest extended states. This relaxation time is directly related to the carrier trapping. The alternative explanation of the fast depopulation dynamics of the extended states by Auger recombination (as proposed in Refs. 22 and 25) is not possible in view of the low excitation densities used in our experiments.

At first sight, the 1-ps trapping disagrees with a subpicosecond buildup of PL related to the localized states ($\hbar\omega < 2.6$ eV). However, these data can be easily understood under the assumption that the cw PL is dominated by the transitions coupling extended states to localized ones; and the localized states are already occupied by carriers (opposite to those in the extended states) in the absence of the pump. The PL rise time for this recombination mechanism is only determined by carrier intraband relaxation rather than by trapping. This explanation is consistent with data of Ref. 26 on PL and differential transmission (DT) in CdSe NC's. Both the PL and the DT spectra reported in this reference were dominated by two bands with the same spacing, which was equal to the energy separation between $1s$ and $1p$ extended electron states. At the same time, the PL bands were redshifted with respect to those in the DT by about 50 meV. This provides evidence for the extended-to-localized state mechanism of the band-edge emission and furthermore shows that the extended states are the electron ones, whereas the localized states are those of the holes. Presumably, the same states are involved in the band-edge emission in CdS NC's studied by us. Note that a similar mechanism of the pump-excited minority carrier recombination with preexisting majority carriers has been previously proposed in Ref. 7 for explanation of the deep-center emission in CdS NC's.

Discussing the nature of the defect states contributing to the band-edge PL, it is natural to consider first surface located native defects such as sulfur or cadmium vacancies or add atoms. The low-energy emission band in CdS NC's has been assigned to a surface sulfur vacancy with a level located ~ 0.7 eV below the conduction band.⁷ A Cd vacancy can create two acceptor states in the energy band gap: One (first ionized) above the valence band and the other (second ionized) below the conduction band.³⁰ The other possible acceptor states are complexes associated with the Cd vacancy, such as a complex with a donor at the next lattice site.³¹ Bulk CdS is an n -type material with a conductivity dominated by foreign donor atoms. However, one may expect a different situation in NC's (at least in a portion of them) with a large number of surface located native defects which can lead to the presence of uncompensated acceptors along with compensated ones.

The uncompensated neutral shallow acceptor (A_1^0 ; see schematic energy diagram in Fig. 6) with a level located 80 meV above the lowest hole extended state can be responsible for the ω_2 emission. The rise time of the conduction-band-acceptor-level recombination is determined only by the population rate of the extended electron state leading to nearly the same or even faster (due to finite hole intraband relaxation time) buildup dynamics than for the emission involving two extended states. This is consistent with the time

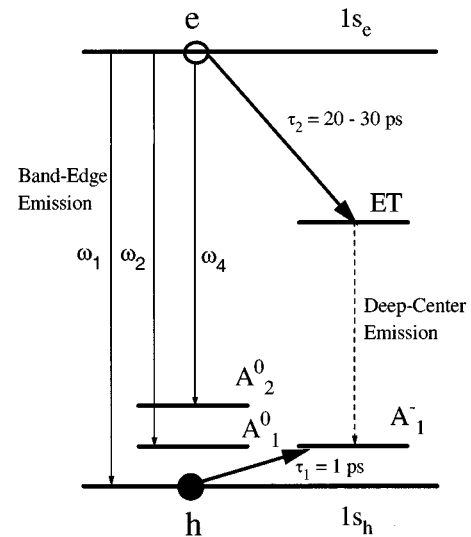


FIG. 6. The tentative scheme of energy levels in a CdS NC which accounts for the PL spectra: $1s_e$ and $1s_h$ are the lowest electron and hole extended states, A^0 and A^- are the levels of the neutral and the charged acceptors, respectively, ET is a deep electron trap. Thin solid and dashed arrows show the transitions leading to the band-edge and the deep-center emission, respectively. Thick solid arrows show the carrier trapping.

transients in Fig. 2 and the data plotted in Fig. 3 which show the slightly faster PL rise time for the ω_2 band than that for the ω_1 band. The difference in relaxation dynamics of the ω_1 and the ω_2 bands can be explained by the slower trapping rate for an electron than for a hole as suggested in Ref. 19. The presence of negatively charged compensated acceptors (A_1^- in Fig. 6) can lead to a fast capture of the photoexcited holes and to the 1-ps decay of the ω_1 band observed experimentally. The 20–30-ps decay of the ω_2 band is probably associated with a capture of an electron by deep centers [electron traps (ET) in Fig. 6] which give rise to the low-energy PL band. This process can evidently explain the relatively slow PL buildup dynamics measured in Ref. 29. Note that a depopulation of the lowest electron state on the time scale of 10 ps has been previously observed in time-resolved DT spectra of CdSe quantum dots.³²

The band ω_4 has the same dynamics as the band ω_2 which may be considered as a hint toward the same mechanism for this emission, namely, the conduction-band-acceptor-level recombination. The acceptor level (A_2^0 in Fig. 6) which could be responsible for this emission has the localization energy of ~ 270 meV. The band ω_3 has much faster relaxation dynamics than those of the ω_2 and ω_4 bands, but slower than that of the ω_1 band. This indicates a presence of at least one more shallow level being involved in the band-edge emission. However, the exact origins of the states involved in the ω_3 emission remain unclear and are under further investigation.

V. CONCLUSIONS

In conclusion, we have studied femtosecond dynamics of the band-edge emission in CdS NC's dispersed in a glass matrix. Time-resolved PL exhibits several discrete features

(not resolved in cw PL) which indicate the presence of shallow localized states in the energy band gap involved in the band-edge emission. The comparison of the cw and the time-resolved PL spectra shows that the cw emission is dominated by the interband transitions coupling the extended to the localized states; and these latter are occupied in the absence of the pump. This explains the extremely fast buildup dynamics (the rise time is 400–700 fs) of the localized-carrier-related emission. Time-resolved PL exhibits a short-lived band at the position of the transition coupling the lowest extended electron and hole states. The decay of this band is explained by a fast capture of one of the carriers (tentatively, a hole) on the time scale of 1 ps. The slower trapping of the other carrier with a time constant of 20–30 ps governs the decay of the emission originating from the extended-to-localized state recombination.

Additionally, the time transients measured indicate a carrier energy-loss rate (intraband relaxation) of 0.7 meV fs^{-1} per e - h pair that exceeds the experimentally measured values for bulk CdS at the same pump intensities. This shows that the 3D confinement results in the reduced efficiency of the high-density effects leading normally to the slowed cooling in bulk polar semiconductors.

ACKNOWLEDGMENTS

The authors thank D. McBranch for critical reading of the manuscript. V.K. acknowledges the support from the Alexander von Humboldt Foundation. P.H. is supported by the Heinrich Hertz Foundation.

-
- *Present address: Chemical Sciences and Technology Division, CST-6, MS-J585 Los Alamos National Laboratory, Los Alamos, NM 87545.
- ¹N. F. Borrelli, D. W. Hall, H. J. Holland, and D. W. Smith, *J. Appl. Phys.* **61**, 5399 (1987).
 - ²R. Rosetti, J. L. Ellison, J. M. Gibson, and L. E. Brus, *J. Chem. Phys.* **80**, 4464 (1984); E. F. Hilinskii, P. A. Lucas, and Y. Wang, *ibid.* **89**, 3435 (1988).
 - ³S. H. Park, R. A. Morgan, Y. Z. Hu, M. Linberg, S. W. Koch, and N. Peyghambarian, *J. Opt. Soc. Am. B* **7**, 2097 (1990); T. Tokizaki, H. Akiyama, M. Takaya, and A. Nakamura, *J. Cryst. Growth* **117**, 603 (1992); W. S. O. Roden, S. M. Sotomayr Torres, C. N. Ironside, D. Cotter, and H. P. Girdlestone, *Superlatt. Microstruct.* **9**, 421 (1991).
 - ⁴Yu. V. Vandyshev, V. S. Dneprovskii, and V. I. Klimov, *Zh. Éksp. Teor. Fiz.* **101**, 270 (1992) [*Sov. Phys. JETP* **74**, 144 (1991)].
 - ⁵Yu. V. Vandyshev, V. S. Dneprovskii, V. I. Klimov, and D. K. Okorokov, *Pis'ma Zh. Éksp. Teor. Fiz.* **54**, 441 (1991) [*JETP Lett.* **54**, 442 (1991)]; V. Dneprovskii, V. Klimov, D. Okorokov, and Yu. V. Vandyshev, *Solid State Commun.* **81**, 227 (1992).
 - ⁶D. J. Norris, A. Sacra, C. B. Murray, and M. G. Bawendii, *Phys. Rev. Lett.* **72**, 2612 (1994); A. I. Ekimov, F. Hache, M. C. Schanne-Klein, D. Ricard, C. Flytzanis, I. A. Kudryavtsev, T. V. Yazeva, A. V. Rodina, and Al. L. Efros, *J. Opt. Soc. Am. B* **10**, 100 (1993); C. Spiegelberg, F. Henneberger, and J. Puls, *Superlatt. Microstruct.* **9**, 487 (1991).
 - ⁷N. Chesnoy, T. D. Harris, R. Hull, and L. E. Brus, *J. Phys. Chem.* **90**, 3393 (1986).
 - ⁸Y. Wang and N. Herron, *J. Phys. Chem.* **92**, 4988 (1988).
 - ⁹M. O'Neil, J. Mahron, and G. McLendon, *J. Phys. Chem.* **94**, 4356 (1990).
 - ¹⁰M. G. Bawendi, P. J. Carroll, W. L. Wilson, and L. E. Brus, *J. Chem. Phys.* **96**, 946 (1992).
 - ¹¹J. P. Zheng, L. Shi, F. S. Choa, P. L. Liu, and H. S. Kwok, *Appl. Phys. Lett.* **53**, 643 (1988).
 - ¹²K. Misawa, H. Yao, T. Hayashi, and T. Kobayashi, *J. Cryst. Growth* **117**, 617 (1992).
 - ¹³T. Inokuma, T. Arai, and M. Ishikawa, *Phys. Rev. B* **42**, 11 093 (1990).
 - ¹⁴A. Uhrig, L. Banyani, S. Gaponenko, A. Wörner, N. Neuroth, and C. Klingshirm, *Z. Phys. D* **20**, 345 (1991).
 - ¹⁵M. G. Bawendi, W. L. Wilson, L. Rothberg, P. J. Carrol, T. M. Jedju, M. L. Steigerwald, and L. E. Brus, *Phys. Rev. Lett.* **65**, 1623 (1990).
 - ¹⁶F. Hache, M. C. Klein, D. Ricard, and C. Flytzanis, *J. Opt. Soc. Am. B* **8**, 1802 (1991).
 - ¹⁷V. S. Dneprovskii, Al. L. Efros, A. I. Ekimov, V. I. Klimov, I. A. Kudryavtsev, and M. G. Novikov, *Solid State Commun.* **74**, 555 (1990); M. Ghanassi, M. C. Schanne-Klein, F. Hache, A. I. Ekimov, D. Ricard, and C. Flytzanis, *Appl. Phys. Lett.* **62**, 78 (1993).
 - ¹⁸M. Tomita and M. Matsuoka, *J. Opt. Soc. Am. B* **7**, 1198 (1990).
 - ¹⁹J. Puls, V. Jungnickel, F. Henneberger, and A. Schülzgen, *J. Cryst. Growth* **138**, 1005 (1994).
 - ²⁰M. C. Nuss, W. Zinth, and W. Kaiser, *Appl. Phys. Lett.* **42**, 1717 (1986).
 - ²¹V. Klimov, S. Hunsche, and H. Kurz, *Phys. Rev. B* **50**, 8110 (1994).
 - ²²J. Z. Zhang, R. H. O'Neil, and T. W. Roberti, *Appl. Phys. Lett.* **64**, 1989 (1994).
 - ²³R. W. Schoenlein, D. M. Mittleman, J. J. Shiang, A. P. Alivisatos, and C. V. Shank, *Phys. Rev. Lett.* **70**, 1014 (1993).
 - ²⁴J. Shah, *IEEE J. Quantum Electron.* **QE-24**, 276 (1988).
 - ²⁵N. P. Ernstring, M. Kaschke, H. Weller, and L. Katsikas, *J. Opt. Soc. Am. B* **7**, 1630 (1990).
 - ²⁶V. S. Dnerovskii, V. A. Karavanskii, and V. I. Klimov, *Fiz. Tverd. Tela (St. Petersburg)* **35**, 2626 (1993) [*Phys. Solid State* **35**, 1297 (1993)].
 - ²⁷V. Klimov, P. Haring Bolivar, and H. Kurz, *Phys. Rev. B* **52**, 4728 (1995).
 - ²⁸W. Pötz and P. Kocevar, *Phys. Rev. B* **28**, 7040 (1983).
 - ²⁹M. O'Neil, J. Marohn, and G. McLendon, *Chem. Phys. Lett.* **168**, 208 (1990).
 - ³⁰M. R. Lorenz and H. H. Woodbury, *Phys. Rev. Lett.* **10**, 215 (1963); M. R. Lorenz and B. Segal, *Phys. Lett.* **7**, 18 (1963).
 - ³¹S. Shionoya, *J. Lumin.* **1,2**, 17 (1970).
 - ³²V. Klimov, S. Hunsche, and H. Kurz, *Phys. Status Solidi B* **188**, 259 (1995).